

# Implementation and study of switched impedance boost and KY-boost converters for electric vehicle

Sapavath Sreenu, J. Upendar, B. Sirisha

Department of Electrical Engineering, University College of Engineering, Osmania University, Hyderabad, India

## Article Info

### Article history:

Received Dec 23, 2022

Revised Jul 15, 2023

Accepted Jul 29, 2023

### Keywords:

DC-DC converter

Electric vehicle

Fuzzy logic controller

KY-boost converter

PV array

ZSC

## ABSTRACT

A DC/DC converter based on photovoltaic (PV) grid connections is proposed here. This work focuses on the switched impedance source (S\_ZSC) for electric vehicles. Every PV grid-connected system require step-up DC/DC converters to boost voltage range from low to high. Connecting an extra diode and a switch to the terminals of a standard quasi-impedance source DC/DC converter raises the step-up factors. In this proposed converter, this capacitor does more than just filter noise. Saturated inductors, on the other hand, can cause instability that needs not occur. In any case, the modulation index's H-bridge at its extremes is adjustable to a broader range when the circuit is used for DC-AC conversion. A larger boost factor is achieved with a shorter duty time as compared to currently available Z-source based systems. Both a buck-boost charging station and a KY-boost charging station were modeled for this investigation. PI or fuzzy logic controllers are utilized in DC-DC converters to keep the output voltage stable.

This is an open access article under the [CC BY-SA](https://creativecommons.org/licenses/by-sa/4.0/) license.



## Corresponding Author:

Sapavath Sreenu

Department of Electrical Engineering, University College of Engineering (A), Osmania University

Amberpet, Hyderabad, Telangana, India

Email: sreenu.ou@osmania.ac.in

## 1. INTRODUCTION

The worldwide shortage of traditional fossil fuels has accelerated the shift toward renewable energy sources [1]–[5]. Solar power has emerged as a major force in the fight against the energy crisis. Low DC voltage from PV arrays necessitates a large step-up ratio in the AC/DC converter used to power grid-connected inverters. Figure 1 shows grid connected switched ZSC/KY-boost converter.

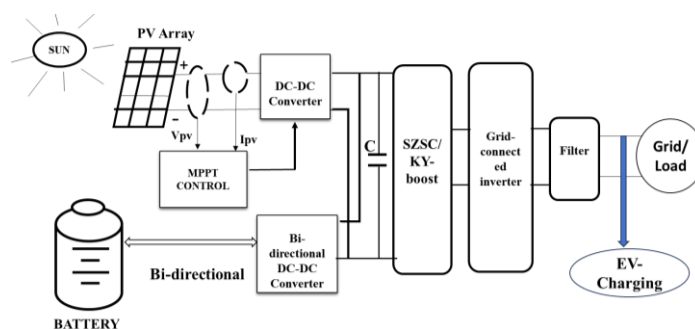


Figure 1. Grid-connected switched ZSC/KY boost converter photovoltaic system for electric vehicle charging

However, larger switching duty cycles are required to attain the high voltage gain, which reduces efficiency and leads to inductor saturation. Quasi impedance source inverters are recommended as a means of overcoming the drawbacks of conventional impedance source inverter (ZSI), such as excessive inrush current, a discontinuous input current, and increased condenser voltage stress. In order to raise the ZSI's boost factor, researchers have experimented with a number of approaches [6]–[11]. Higher DC-link voltage is produced, for instance, when capacitors, inductors, and diodes are all coupled to the Z-source network [12]–[15].

The topology employs a cascaded qZ-source network to increase voltage gain [16]. Figure 2 depicts the switched-Z-source DC/AC inverter. Since the front-end switched-Z-source network has a boost factor of  $1/(1-4D)$ , a high voltage gain is possible at a low duty cycle. The index of the H-modulation bridge at the back end, consequently, has a greater range of adjustment [17].

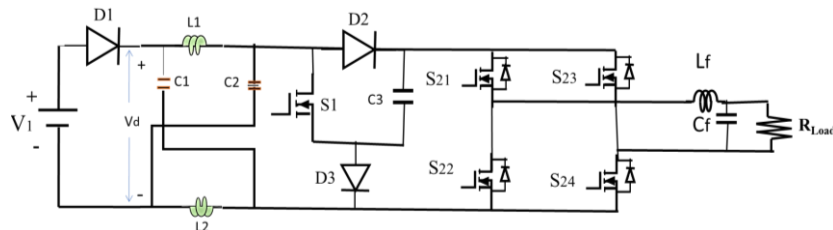


Figure 2. The suggested DC/AC inverter switched impedance source circuit topology

## 2. KY BOOST CONVERTER

When combined with a standard “synchronously-rectified boost-converter,” as in [18], the KY-converter becomes a voltage boost-converter known as a “KY boost-converter,” where the voltage ratio is significantly increased. Additionally, this converter is exceptional since it not only operates in CCM continuously, but also has independent input and output inductors, reducing current ripples to a minimum.

The suggested “KY boost converter,” which combines a “KY-converter” and a “standard SR-boost-converter,” is seen in Figure 3. “Kentucky-boost” condenser part of it is the switches. S2 and S1, the diode Db, the energy-transfer capacitor Cb, the load-side inductor Lo, and the load-side capacitor Co [19]. In addition, one buffer capacitor-Cm is used in place of the KY converter's input. As an alternative, a traditional “SR-boost converter” consists of switches S2 and S1 and the input-inductor (Li). On top of that, the output of the replacement for the standard SR boost converter with the output of the KY-converter, which is buffered by the capacitor (Cm). The output load is symbolized by a single load resistor RL [20].

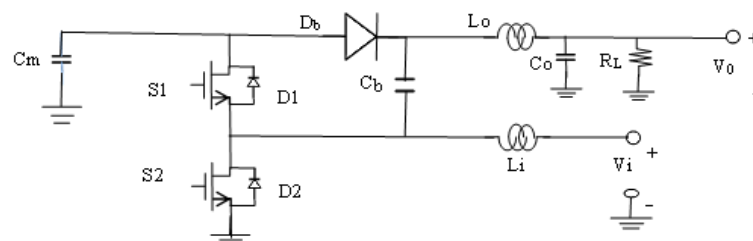


Figure 3. KY boost converter

These are some of the most important presumptions: i) All electronic power switches operate instantly; ii) During the on-state, no voltage is lost through the switch or diodes; iii) To indicate the direction of the current flowing through the inductors Lo and Li, we used the symbols  $iL_0$  and  $iL_i$ ; and iv) Cb, energy storage capacitor that uses the “charge pump” principle, is rapidly excited by  $V_{Cm}$  for a short duration, much less than the switching period Ts [21].

D1 diode of the S1 switch excites capacitor Cm almost instantly after the KY Boost-converter receives its power from the DC-voltage source. Afterwards, the “pulse width modulated” gate pulses are generated and sent to the switch. Switch S2 is on, therefore the capacitor Cb is being charged at the present voltage setting (Cm). The converter stabilizes after a number of switching cycles.

Since it is a single-stage DC-DC converter that incorporates both the “SR boost-converter” and the “KY-converter,” it operates in continuous current mode (CCM) at all times when operating in the high-

voltage range though the inductor currents may be either negative or positive, their net effect is positive, indicating a continuous transfer of energy from the source to the load [22].

Therefore, the converter can be used in two distinct modes: in mode 1, the switches are on for a period of time equal to (1-D), whereas in mode 2, the duty cycles are (D) and (1-D), respectively. In addition, when everything is functioning well, the voltage at (Cm) is nearly identical to the value at (Cb).

- Mode 1

S2 is active while S1 is inactive in Figure 4. Because Db is now forward biased and conducting, the Cb cathode terminal will be dragged to ground potential. While the Cb is being charged, the Cm is being de-energized. Li has a voltage of Vi, causing it to become magnetized, while Lo has a voltage of VO-VCm, causing it to undergo discharge. More so, the current via Co changes to iLo iRL, whereas the current through Cm is the sum of the currents through -iCb and -iLo [23].

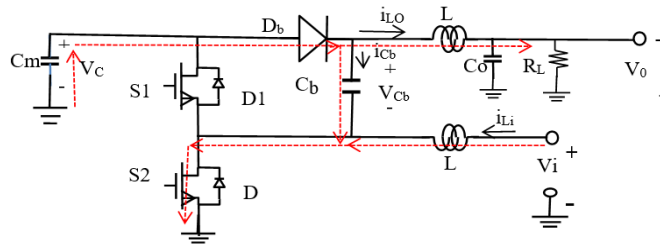


Figure 4. Flow of power in mode 1

- Mode 2

Referring to Figure 5, switch S1 on and S2 off. Given that S1 is active right now, turning off Db makes sense. In this state, Cm is energized while Cb is de-energized. Since at Li, the voltage was Vi-Vcm, Li became uncharged, but the voltage at Lo was 2Vcm - VO, magnetization occurred at Lo. In addition, iLo-iRL equals the current through Co, but iLi-iLo equals the current through Cm [24], [25]. That's why the output voltage of a “KY boost-converter” is to the input voltage in the following ratio:

$$\frac{V_o}{V_i} = \frac{2 - D}{1 - D}$$

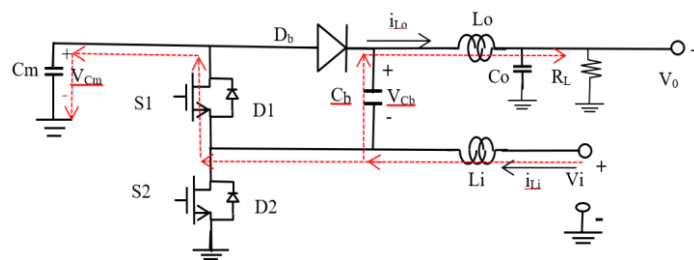


Figure 5. Mode 2 power flow

### 3. IMPEDANCE NETWORK MATHEMATICAL ANALYSIS

Assuming the capacitors (C1 and C2) and inductors (L1 and L2) are both at their nominal values, we can proceed. Voltage at input Vd, voltage at discharge Vi, L1 and L2 inductors in series, C1 and C2 capacitors in parallel. From the data presented in Figure 6, an equivalent circuit model of an impedance source inverter may be constructed in (1)-(12).

$$V_{Cap1} - V_{Cap2} = V_{Cap} \tag{1}$$

$$V_{Cap1} - V_{Cap2} = V_{Cap} \tag{2}$$

$$V_{Ind} = V_{Cap}, V_D = 2V_{Cap} \text{ and } V_I = 0$$

$$\text{At Switching cycle } T, V_{Ind} = V_0 - V_{Cap} \quad (3)$$

$$V_D = V_0 \text{ and } V_I = V_{Cap} - V_{Ind} = 2V_{Cap} - V_0 \quad (4)$$

Where:

$$T = T_0 + T_1 \quad (5)$$

and the DC source voltage is  $V_0$ .

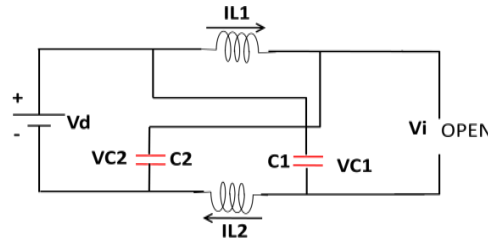


Figure 6. Impedance inverter equivalent circuit

After one cycle of switching, the inductors' average voltage should be zero at steady state ( $T$ ).

$$V_{Ind} = \frac{T_0 \cdot V_{Cap} + T_1 (V_0 - V_{Cap})}{T} = 0$$

$$\frac{V_{Cap}}{V_0} = \frac{T_1}{T_1 - T_0} \quad (6)$$

A similar equation can be used to calculate typical DC voltage at the inverter bridge (4).

$$V_I = (T_0 * 0 + T_1) * \frac{2V_{Cap} - V_0}{T} \quad (7)$$

From in (6)  $T_1 * \frac{V_1}{T_1 - T_0} = 2V_{Cap} \cdot T_1 / (T_1 - T_0)$

$$V_{Cap} = V_0 * T_1 / (T_1 - T_0)$$

An inverter bridge's DC-link voltage can't go any higher than,  $V_I = V_{Cap} - V_{Ind} = 2V_{Cap} - V_0$ .

$$= T / (T_1 - T_0) * V_0 = B * V_0 \text{ here } B = T / (T_1 - T_0) \text{ i. e.} \quad (8)$$

- Boost factories B

At the inverter's output, the highest phase voltage is

$$V_{ac} = M * V_i / 2, \quad (9)$$

Modulation index is M in this case, and the voltage source

$$V_{ac} = M * B * \frac{V_0}{2} \quad (10)$$

One can step down and up the  $V_0$  before settling on a suitable buck-boost factor (BB)

$$B.B = B * M \text{ (range from 0 to 1)} \quad (11)$$

Voltage across the capacitor is

$$V_{cap1} = V_{cap2} = V_{cap} = (1 - T_0/T) * V_0 / (1 - 2T_0/T) \quad (12)$$

**4. WORKING PRINCIPLE AND TOPOLOGIES OF THE PROPOSED CONVERTERS**

Since the three proposed circuits have identical circuit layouts, the following simulation will focus mostly on the first network, switched-ZSC. It is possible to apply the same method to assess the other two SQZSCs listed below. In either the common current mode (CCM) or the differential current mode (DCM), the critical current mode (CCM) is a subset. While two different cases (Cases 1&2) may show up in CCM depending on the values of inductance, duty cycle, and load resistance, only case 3 may show up in discontinuous conduction mode. At any one time, each individual circuit in a loop will be in a distinct state. The two modes represented in Figures 7(a)-7(c) contain all of the circuit's states (e). In Figure 7(a) the reference directions for each variable are shown Case 1-State1 to State2; Case 2-State1 to State2 to State3; Case 3- State1 to State2 to State 3; Here, KVL can be used to determine the voltages across all three capacitors. State1 to State2 to State3 to State4. For the sake of simplicity, assuming: 1) All ideal power components; 2)  $L_1 = L_2$  and  $C_1 = C_2$  are ignored; and 3)  $L_1 = L_2$  and  $C_1 = C_2$ . The current loop for state1 is shown in Figure 7(b), where equal current flows via  $L_1$  and  $C_1$ . Current flow for state2 is shown in Figure 7(c). The flow of currents in state 3 is shown in Figure 7(d), while the flow of currents in state 4 is shown in Figure 7(e).

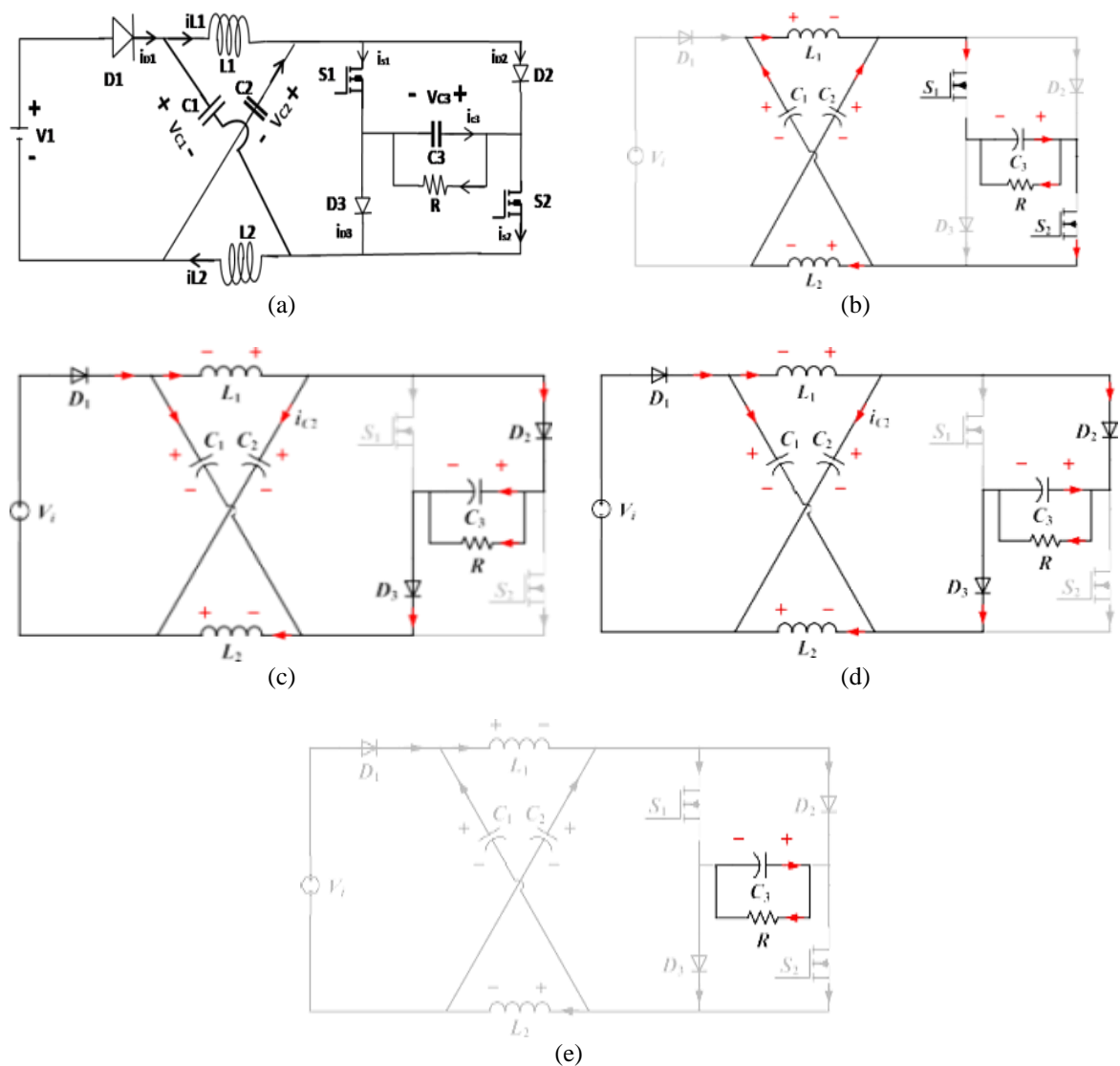


Figure 7. Different states of proposed SZSC: (a) specification of reference directions, (b) current loop of the proposed SZSC in State1: S1 and S2 on; D1, D2 and D3 off, (c) current loop of the proposed SZSC in State2: D1, D2 and D3 on; S1 and S2 off, (d) current loop of the proposed SZSC in State3: D1, D2 and D3on; S1 and S2 off, and (e) the proposed SZSC' current loop in State4 is as follows: S1, S2, D1, D2, and D3 are all turned off

## 5. SIMULATION RESULTS

### 5.1. Switched impedance source converter

When connecting four PV panels in series, the resulting voltage is 215V dc, which is perfect for a 100 V DC/AC converter. From these prior investigations, we get the following values for the simulation's inputs: i)  $V_i$  is 68 volts; ii)  $f_s$  is 25 kHz; with a 0.2 service interval, iii) As predicted, the evaluated output power is 185 W, iv)  $L_1=L_2=320\mu\text{H}$ , include resistance to parasites of 28-m $\Omega$ ; v)  $C_1=C_2=C_3=330\ \mu\text{F}$ , with a sequence resistance of 10-m $\Omega$  equivalent; vi) Resistance in the on position of switches S1 and S2 is 14.5-m $\Omega$ ; vii) The diodes D1, D2, and D3 have a forward voltage drop of 1 V. Figure 8 illustrate the voltage across capacitors and the current through the inductor input are both simulated in switched buck converters. As can be seen in Figure 9, the voltage, current, and power waveforms of the proposed CSQZSC follow the MPPT model for P&O operation.

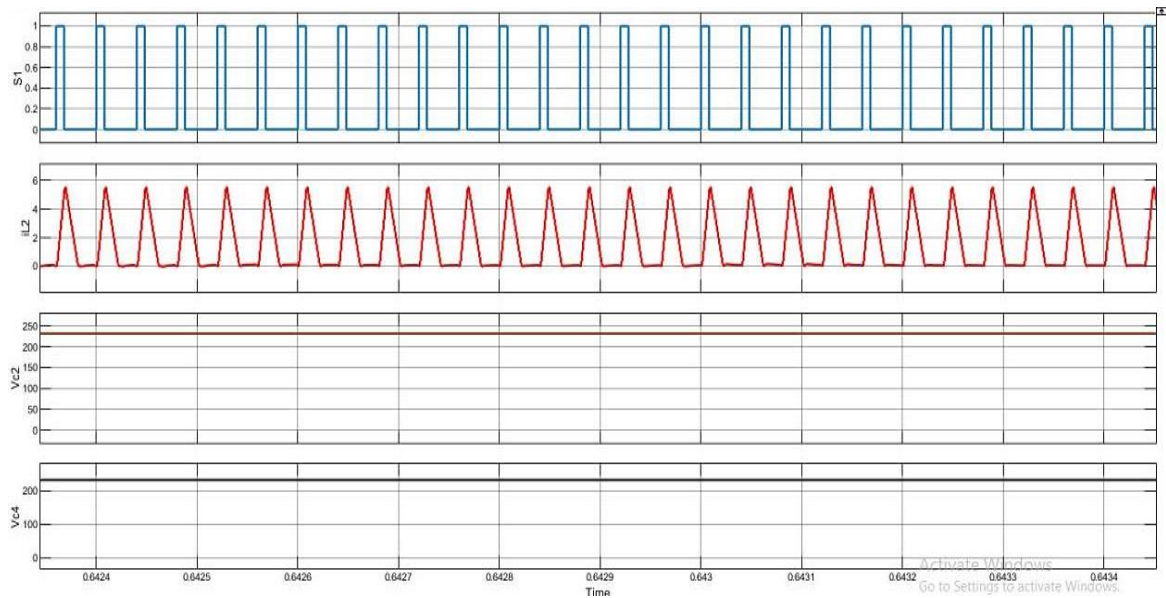


Figure 8. The proposed SZSC's simulation waveforms at 0.2 duty cycle, GatesignalS1,  $i_{L1}$ ,  $v_{C2}$  and  $v_{C4}$  ( $v_{C2}=v_{C4}=215\text{v}$ )

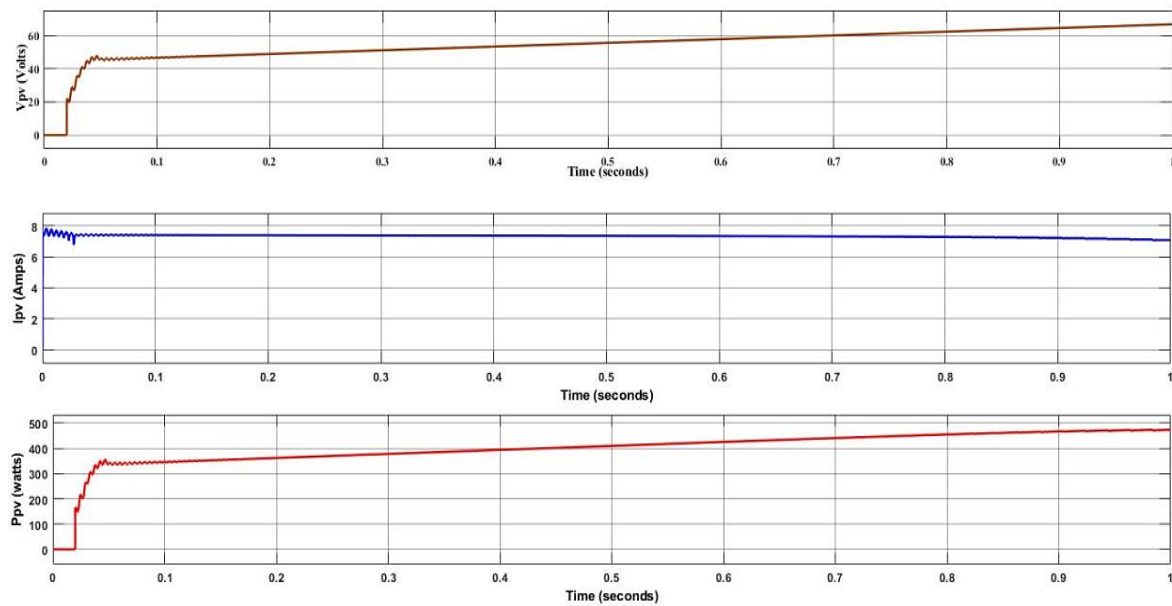


Figure 9. The simulation wave forms of P&O MPPT based behavior of PV voltage, current and power

As can be seen in Figure 10(a), the SOC (percentage) of the battery is 79.99 at the given time in seconds. Inductor operation depicted in Figure 10(b) with current discharged from 250 A to -0.5 A. Figure 10 (b). The time-dependent voltage across the 52 V inductor is depicted in Figure 10(c).

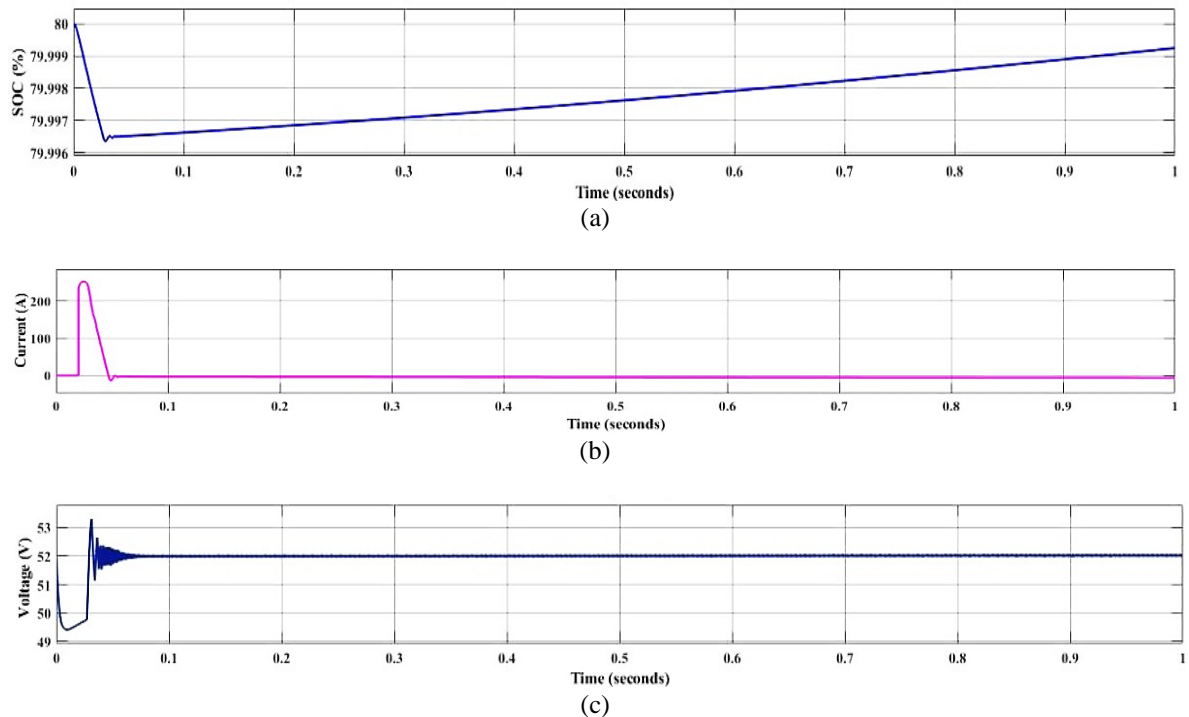


Figure 10. Simulation waveforms of battery (a) SOC (%), (b) voltage, and (c) current

## 5.2. KY-boost converter with PI-controller

From the “three phase thyristor bridge rectifier” output, seven paralleled KY-boost converters were fed. Every one of the seven EV batteries is supplied by a different KY-boost converter, which regulates the DC output voltage. The Figure 11 (see Appendix) shows the Simulink diagram of PI control circuit of KY-boost converter and results of battery output, voltage and current characteristics.

## 5.3. KY-boost converter controlled with fuzzy logic controller

The output voltage of “three phase thyristor bridge rectifier” was given to seven parallel-connected KY-boost converters. Every one of the seven EV batteries is supplied by a different KY Boost converter, which regulates the DC output voltage. Fuzzy logic controls the KY Boost converter's operation. The Figure 12 (see Appendix) shows the Simulink diagram of Fuzzy control circuit of KY-boost converter and results of Battery output, voltage and current characteristics.

## 6. CONCLUSION

It is proposed that a new line of switched impedance source S\_ZSCs with a slightly different architecture be created for PV applications. Normal ZS dc/dc converters can have their boost factors boosted to 1 by adding an extra switch and diode (1-4D). High voltage gain can be achieved by using a short duty cycle, which also prevents instabilities caused by inductor saturation. Both the suggested converters and the hybrid three Z-network boost converters have the same boost ratio. That were just suggested, but with less passive parts, resulting in greater power density and less per-unit prices. In terms of voltage and current, the THD of battery pack with the KY Boost-converter controlled by the “fuzzy-logic controller” has the least harmonic contamination, so it is preferable to have the charger with the KY-boost converter was in charge of by the “fuzzy-logic controller”. Consequently, the “KY boost-converter” controlled by the “Fuzzy logic controller” has the lowest total harmonic distortion (THD), whereas the “buck-boost converter” controlled by the “proportional and integral controller” or the “fuzzy logic controller” has the highest THD. In this work, we examine the fundamentals of these devices' operation, including their current, voltage, and efficiency of

conversion due to parasitic factors. In the end, simulation findings corroborated the aforementioned features and theoretical analyses.

**APPENDIX**

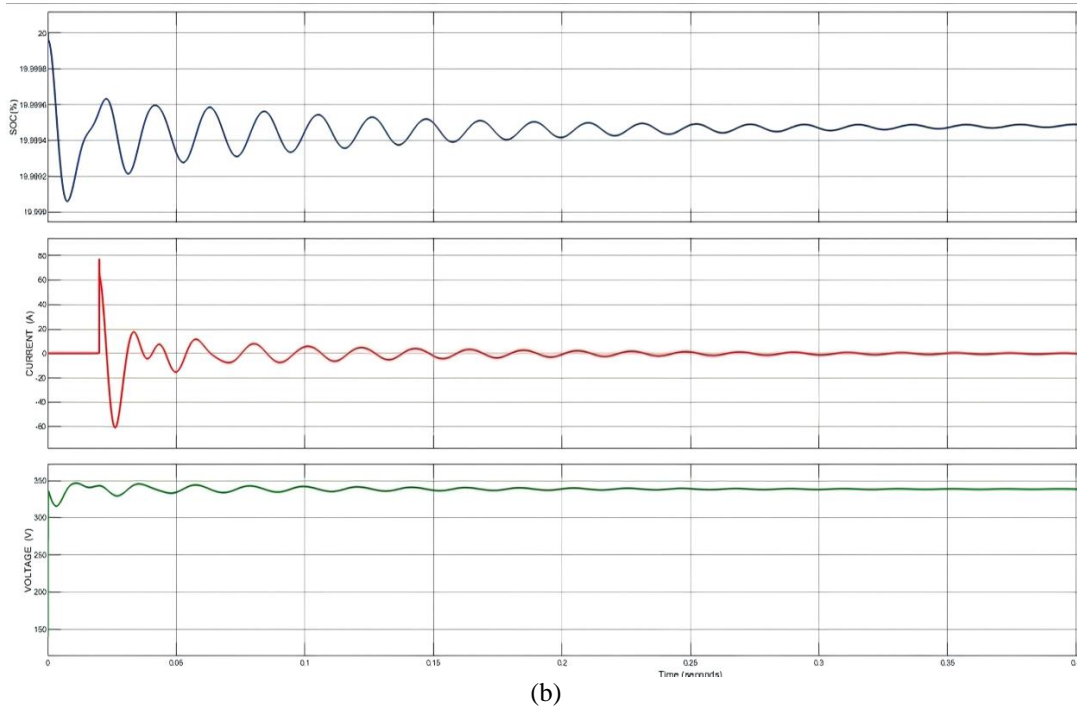
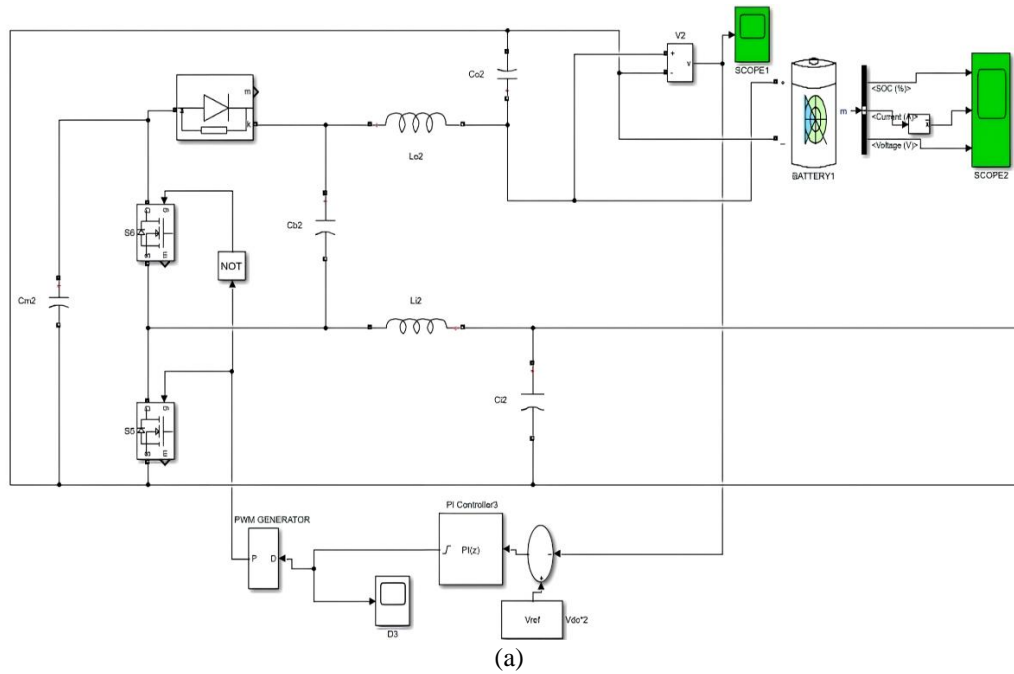


Figure 11. MATLAB Simulink block and results of KY boost converter (a) PI control model simulation in MATLAB/Simulink and (b) battery output SOC (%), voltage, and current characteristics

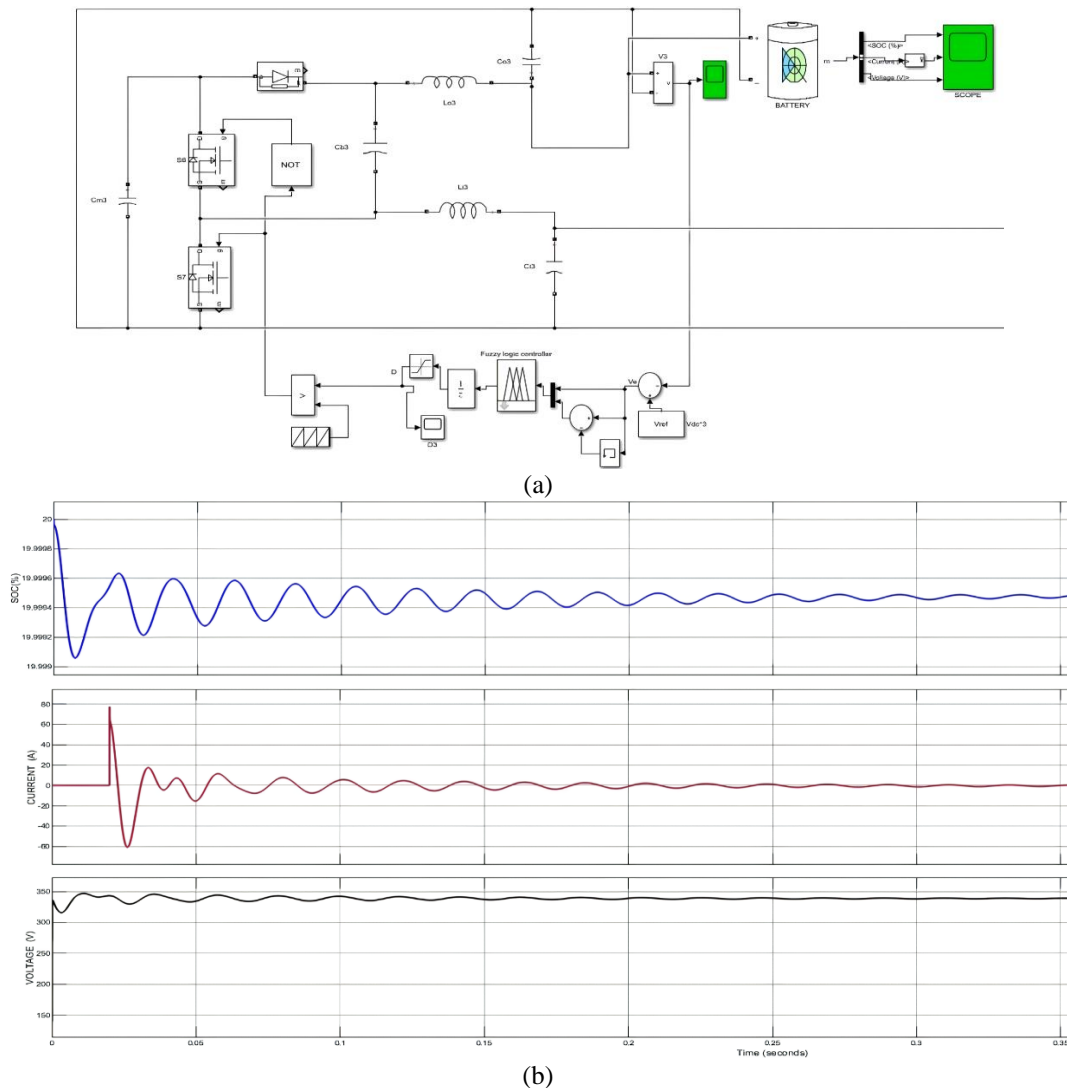


Figure 12. MATLAB/Simulink block and results of KY boost converter (a) fuzzy control model simulation in MATLAB/Simulink and (b) battery output SOC (%), voltage and current characteristics

## REFERENCES

- [1] N. Javaid *et al.*, "An Intelligent Load Management System with Renewable Energy Integration for Smart Homes," *IEEE Access*, vol. 5, pp. 13587–13600, 2017, doi: 10.1109/ACCESS.2017.2715225.
- [2] H. Suryatomo *et al.*, "Design of MPPT based fuzzy logic for solar-powered unmanned aerial vehicle application," *ICEAST 2018 - 4th International Conference on Engineering, Applied Sciences and Technology: Exploring Innovative Solutions for Smart Society*, 2018, doi: 10.1109/ICEAST.2018.8434430.
- [3] S. Sreenu, J. Upendar, and B. Sirisha, "Analysis of switched impedance source/quasi-impedance source DC-DC converters for photovoltaic system," *International Journal of Applied Power Engineering*, vol. 11, no. 1, pp. 14–24, 2022, doi: 10.11591/ijape.v11.i1.pp14-24.
- [4] J. Upendar, S. R. Kumar, S. Sreenu, and B. Sirisha, "Implementation and study of fuzzy based KY boost converter for electric vehicle charging," *International Journal of Applied Power Engineering (IJAPE)*, vol. 11, no. 1, p. 98, Mar. 2022, doi: 10.11591/ijape.v11.i1.pp98-108.
- [5] W. Tushar, J. A. Zhang, C. Yuen, D. B. Smith, and N. Ul Hassan, "Management of Renewable Energy for a Shared Facility Controller in Smart Grid," *IEEE Access*, vol. 4, pp. 4269–4281, 2016, doi: 10.1109/ACCESS.2016.2592509.
- [6] G. Zhang, B. Zhang, Z. Li, D. Qiu, L. Yang, and W. A. Halang, "A 3-Z-network boost converter," *IEEE Transactions on Industrial Electronics*, vol. 62, no. 1, pp. 278–288, 2015, doi: 10.1109/TIE.2014.2326990.
- [7] B. Axelrod, Y. Berkovich, and A. Ioinovici, "Switched-Capacitor/Switched-Inductor Structures for Getting Transformerless Hybrid DC-DC PWM Converters," *IEEE Transactions on Circuits and Systems I: Regular Papers*, vol. 55, no. 2, pp. 687–696, Mar. 2008, doi: 10.1109/TCSI.2008.916403.
- [8] Y. Tang, T. Wang, and Y. He, "A switched-capacitor-based active-network converter with high voltage Gain," *IEEE Transactions on Power Electronics*, vol. 29, no. 6, pp. 2959–2968, 2014, doi: 10.1109/TPEL.2013.2272639.
- [9] R. J. Wai, C. Y. Lin, R. Y. Duan, and Y. R. Chang, "High-efficiency dc-dc converter with high voltage gain and reduced switch stress," *IEEE Transactions on Industrial Electronics*, vol. 54, no. 1, pp. 354–364, 2007, doi: 10.1109/TIE.2006.888794.
- [10] M. Zhu, T. Wang, and F. L. Luo, "Analysis of voltage-lift-type boost converters," *Proceedings of the 2012 7th IEEE Conference on Industrial Electronics and Applications, ICIEA 2012*, pp. 214–219, 2012, doi: 10.1109/ICIEA.2012.6360725.

- [11] M. Prudente, L. L. Pfitscher, G. Emmendoerfer, E. F. Romaneli, and R. Gules, "Voltage multiplier cells applied to non-isolated DC-DC converters," *IEEE Transactions on Power Electronics*, vol. 23, no. 2, pp. 871–887, 2008, doi: 10.1109/TPEL.2007.915762.
- [12] F. Z. Peng, "Z-source inverter," *IEEE Transactions on Industry Applications*, vol. 39, no. 2, pp. 504–510, Mar. 2003, doi: 10.1109/TIA.2003.808920.
- [13] J. Anderson and F. Z. Peng, "Four quasi-Z-Source inverters," *PESC Record - IEEE Annual Power Electronics Specialists Conference*, pp. 2743–2749, 2008, doi: 10.1109/PESC.2008.4592360.
- [14] Y. Tang, S. Xie, C. Zhang, and Z. Xu, "Improved Z-source inverter with reduced Z-source capacitor voltage stress and soft-start capability," *IEEE Transactions on Power Electronics*, vol. 24, no. 2, pp. 409–415, 2009, doi: 10.1109/TPEL.2008.2006173.
- [15] M. Zhu, K. Yu, and F. L. Luo, "Switched inductor Z-source inverter," *IEEE Transactions on Power Electronics*, vol. 25, no. 8, pp. 2150–2158, 2010, doi: 10.1109/TPEL.2010.2046676.
- [16] M. K. Nguyen, Y. C. Lim, and G. B. Cho, "Switched-inductor quasi-Z-source inverter," *IEEE Transactions on Power Electronics*, vol. 26, no. 11, pp. 3183–3191, 2011, doi: 10.1109/TPEL.2011.2141153.
- [17] R. Sankar and D. Sarala, "Design and implementation of improved Z-source inverter fed induction motor for wind applications," *2017 International Conference on Energy, Communication, Data Analytics and Soft Computing, ICECDS 2017*, pp. 3665–3670, 2018, doi: 10.1109/ICECDS.2017.8390147.
- [18] H. Zhang, "Impact of Current Ripple on Electric Vehicle Charging Equipment," *International Conference on Civil, Transportation and Environment*, Atlantis Press, 2016. doi: 10.2991/iccte-16.2016.161.
- [19] E. W. C. Lo, D. Sustanto, and C. C. Fok, "Harmonic load flow study for electric vehicle chargers," *Proceedings of the International Conference on Power Electronics and Drive Systems*, vol. 1, pp. 495–500, 1999, doi: 10.1109/peds.1999.794613.
- [20] P. T. Staats, W. M. Grady, A. Arapostathis, and R. S. Thallam, "A statistical analysis of the effect of electric vehicle battery charging on distribution system harmonic voltages," *IEEE Transactions on Power Delivery*, vol. 13, no. 2, pp. 640–646, Apr. 1998, doi: 10.1109/61.660951.
- [21] W. Yang, J. Wang, Z. Zhang, and Y. Gao, "Simulation of electric vehicle charging station and harmonic treatment," *2012 International Conference on Systems and Informatics, ICSAI 2012*, pp. 609–613, 2012, doi: 10.1109/ICSAI.2012.6223071.
- [22] R. Mkhail, A. Nait-Sidi-Moh, and M. Wack, "Modeling and Simulation of Standalone Photovoltaic Charging Stations for Electric Vehicles," *International Journal of Computer and Information Engineering*, vol. 9, no. 1, pp. 72–80, 2015, doi: 10.5281/zenodo.1099020.
- [23] M. Utakrue and K. Hongesombut, "Impact Analysis of Electric Vehicle Quick Charging to Power Transformer Life Time in Distribution System," *ITEC Asia-Pacific 2018 - 2018 IEEE Transportation Electrification Conference and Expo, Asia-Pacific: E-Mobility: A Journey from Now and Beyond*, 2018, doi: 10.1109/ITEC-AP.2018.8433281.
- [24] J. A. P. Lopes, F. J. Soares, and P. M. R. Almeida, "Integration of electric vehicles in the electric power system," *Proceedings of the IEEE*, vol. 99, no. 1, pp. 168–183, 2011, doi: 10.1109/JPROC.2010.2066250.
- [25] L. Cheng, B. Wu, H. Chen, W. Ma, and G. Zhang, "Load Forecasting and Harmonic Analysis for EV Charging Station," In *2018 IEEE Innovative Smart Grid Technologies-Asia (ISGT Asia)*, pp. 139–144. IEEE, 2018, doi: 10.1109/ISGT-Asia.2018.8467908.

## BIOGRAPHIES OF AUTHORS



**Sapavath Sreenu**    is Research scholar at the Department of Electrical Engineering, University college of Engineering, Osmania university, Hyderabad, India. He received Master of Technology (M.Tech.) in Power Electronics and Electrical Drives (PE & ED) from Anurag Engineering College (Autonomous), Kodad, India in 2014. And He received Bachelor of Technology (B.Tech.) in Electrical and Electronics Engineering, SRREC in 2010. He can be contacted at email: sreenu06274@gmail.com.



**J. Upendar**    is Assistant Professor at the Department of Electrical Engineering, University college of Engineering, Osmania university, Hyderabad, India, where he has been a faculty member since 2013. From 2010-2013, he was also the Senior Engineer-Power Electronics Team Development, General Electric (GE Power Conversion) (CVT EDC Private Limited) Chennai-32, India (& in UK, France), And completed his Doctor of Philosophy (Ph.D.) in Electrical Engineering from Indian Institute of Technology (IIT), Roorkee, India. His research interests are primarily in the area of intelligent approach for fault classification of power transmission systems, where he is the author/co-author of over 30 research publications. He can be contacted at email: dr.8500003210@gmail.com.



**B. Sirisha**    holds a B.E. in Electrical Engineering from Osmania University, M.Tech. Power Electronics from JNTUH in 2003, and a Ph.D. degree from Osmania University 2018. She has over 16 years of experience in research and teaching and is currently employed as an Associate Professor in Electrical Department, Engineering College, Osmania University, Hyderabad, India. She has published various articles in international and national journal publications and conferences. Multilevel Inverters, power electronics and drives, renewable energy applications and special electrical machines are among her research interests. Osmania University awarded her a Ph.D. in the field of multilevel inverters. She can be contacted at email: sirishab2007@yahoo.com.